CATO-2 Deliverable WP3.03-D23

Case study on reservoir/caprock deformation, surface deformation, seal integrity, and fault reactivation/seismic risk

Prepared by: B. Orlic,
J.H. ter Heege

Reviewed by: C.J. Spiers

Approved by: J. Brouwer
(CATO-2 Director)

1 Executive Summary (restricted)

This report represents the final deliverable D23 of the WP 3.3 “*Caprock and Fault Integrity*” of the CATO-2 project. The deliverable is related to development of the geomechanical modelling capabilities and their application to site-specific reservoir-seal systems.

Geomechanical simulations were conducted on a number of site-specific numerical models of depleted gas fields considered for CO_2 storage in the Netherlands. Simulations were aimed at assessing the maximum areal extent of stress perturbation around depleted reservoirs at the end of depletion period. Simulation results indicate that the extent of stress changes around depleted reservoirs is at least one order of magnitude smaller compared to the extent of stress changes associated with industrial-scale CO_2 storage in saline aquifers. In the case of small compartmentalized gas reservoirs, a few to ten kilometers long and a few kilometers wide, without aquifer support or without pressure drop in supporting aquifers, the maximum extent of stress changes is limited to a few kilometers. On the other hand, the extent of the area affected by pressure perturbations and, consequently, stress perturbations in the case of CO_2 storage in saline aquifers is commonly a few tens to hundreds of kilometers away from the injection zone. The magnitude and pattern of induced stress changes around depleted reservoirs depend on many factors including the structural setting, reservoir shape and the geomechanical rock properties of different lithostratigraphic units.

Distribution List

(this section shows the initial distribution list)

External	Copies	Internal	Copies

Document Change Record

(this section shows the historical versions, with a short description of the updates)

Version	Nr of pages	Short description of change	Pages
2013-05-12	20	Version 1	1-20

Table of Content

1 Executive Summary (restricted) 2
2 Applicable/Reference documents and Abbreviations 4
2.1 Applicable Documents 4
2.2 Reference Documents 4
2.3 Abbreviations 4
3 General Text 5
3.1 Introduction 5
3.2 Paper prepared for the 47th US Rock Mechanics/ Geomechanics Symposium 6

2 Applicable/Reference documents and Abbreviations

2.1 Applicable Documents

(Applicable Documents, including their version, are documents that are the "legal" basis to the work performed)

	Title	**Doc nr**	**Version**
AD-01d	Toezegging CATO-2b	FES10036GXDU	2010.08.05
AD-01f	Besluit wijziging project CATO2b	FES1003AQ1FU	2010.09.21
AD-02a	Consortium Agreement	CATO-2-CA	2009.09.07
AD-02b	CATO-2 Consortium Agreement	CATO-2-CA	2010.09.09
AD-03g	Program Plan 2013	CATO2-WP0.A-D03	2013.04.01

2.2 Reference Documents

(Reference Documents are referred to in the document)

	Title	**Doc nr**	**Version/issue**	**Date**

2.3 Abbreviations

(this refers to abbreviations used in this document)

3 General Text

3.1 Introduction

This report represents the final deliverable D23 of the WP 3.3 "*Caprock and Fault Integrity*" of the CATO-2 project. The deliverable addresses the activities described in task T3.3.1 "*Geomechanical evolution of the reservoir-seal system and induced deformation*". The objectives of this task, according to the CATO-2 Program plan, are as follows:

- Development of numerical modelling capability allowing prediction of the stress-strain evolution in and around a generic reservoir-seal system.
- Application to specific sites to evaluate reservoir deformation, caprock deformation and surface displacements.
- Application to specific sites to evaluate the reactivation and seismic risk potential of pre-existing faults.

The work and results of task T3.3.1 are presented in Chapter 3.2 in the form of the following paper:

- Orlic, B. 2013. Site-specific geomechanical modeling for predicting stress changes around depleted gas reservoirs considered for CO_2 storage in the Netherlands. In *Proceedings of the 47th US Rock Mechanics/ Geomechanics Symposium* held in San Francisco, 23-26 June 2013. Paper no ARMA 13-446.

The work performed in task T3.3.1 by TNO is in agreement with the CATO-2 Program plan.

3.2 Paper prepared for the 47th US Rock Mechanics/ Geomechanics Symposium

The paper has been accepted for presentation at the 47th US Rock Mechanics/ Geomechanics Symposium to be held in San Francisco, 23-26 June 2013 (paper no ARMA 13-446)

ARMA 13-446

Site-specific geomechanical modeling for predicting stress changes around depleted gas reservoirs considered for CO_2 storage in the Netherlands

Orlic, B.
TNO, Earth, Environmental and Life Sciences, Utrecht, The Netherlands

This paper was prepared for presentation at the 47th US Rock Mechanics / Geomechanics Symposium held in San Francisco, CA, USA, 23-26 June 2013.

ABSTRACT: Geomechanical simulations were conducted on a number of site-specific numerical models of depleted gas fields considered for CO_2 storage in the Netherlands. Simulations were aimed at assessing the maximum areal extent of stress perturbation around depleted reservoirs at the end of depletion period. Simulation results indicate that the extent of stress changes around depleted reservoirs is at least one order of magnitude smaller compared to the extent of stress changes associated with industrial-scale CO_2 storage in saline aquifers. In the case of small compartmentalized gas reservoirs, a few to ten kilometers long and a few kilometers wide, without aquifer support or without pressure drop in supporting aquifers, the maximum extent of stress changes is limited to a few kilometers. On the other hand, the extent of the area affected by pressure perturbations and, consequently, stress perturbations in the case of CO_2 storage in saline aquifers is commonly a few tens to hundreds of kilometers away from the injection zone. The magnitude and pattern of induced stress changes around depleted reservoirs depend on many factors including the structural setting, reservoir shape and the geomechanical rock properties of different lithostratigraphic units.

1. INTRODUCTION

The Netherlands is the largest producer of natural gas in the European Union. Two-third of production volumes come from the gigantic Groningen gas field and one third from over 190 smaller gas fields. Many of these small fields are nowadays in the mature production phase, or already fully depleted. Over the last decade several studies were conducted to assess the feasibility of CO_2 storage in some of the depleted gas fields. A list of the sites considered for CO_2 storage is given on the website of the national research program for CO_2 Capture, Transport and Storage in the Netherlands (CATO-2) [1].

We evaluated the geomechanical effects associated with past gas extraction and future CO_2 injection in several recently accomplished feasibility studies of geological CO_2 storage in depleted gas fields. The aim of these geomechanical studies, often called *Caprock and fault integrity studies,* was to assess the mechanical effects of reservoir depletion and CO_2 injection on the integrity of top seals and fault stability. Such an assessment allows defining the geomechanical constraints for safe CO_2 injection and storage [e.g. 2, 3].

In this paper we use a number of site-specific numerical models, developed in the course of feasibility studies for CO_2 storage in the Netherlands, to determine the spatial extent of induced stress changes around depleted gas reservoirs. The focus of the present study is to estimate the size of the area (i.e. volume) around depleting gas reservoirs affected by the largest induced stress changes, which occur at the end of depletion period. Assessing the impact of induced stresses on the reservoir-caprock-fault system is beyond the scope of this paper.

The outcome of the present study will demonstrate that the extent of depletion-induced stress changes around the studied gas reservoirs considered for CO_2 storage is much smaller than in the case of industrial-scale CO_2 storage in saline aquifers. In the latter case, considerable pressure build-up and associated stress changes can affect an area tens to hundreds of kilometers away from the injection zone [e.g. 4, 5, 6].

The sites discussed here include (Table 1):

- **(i)** Two depleted gas fields located close to the Port of Rotterdam (field A [7, 8] and field B [9] in Fig. 1).
- **(ii)** Two depleted hydrocarbon fields located in the Dutch North Sea in blocks Q8 (field C in Fig. 1) and P18 (field D in Fig. 1 [6, 10]).

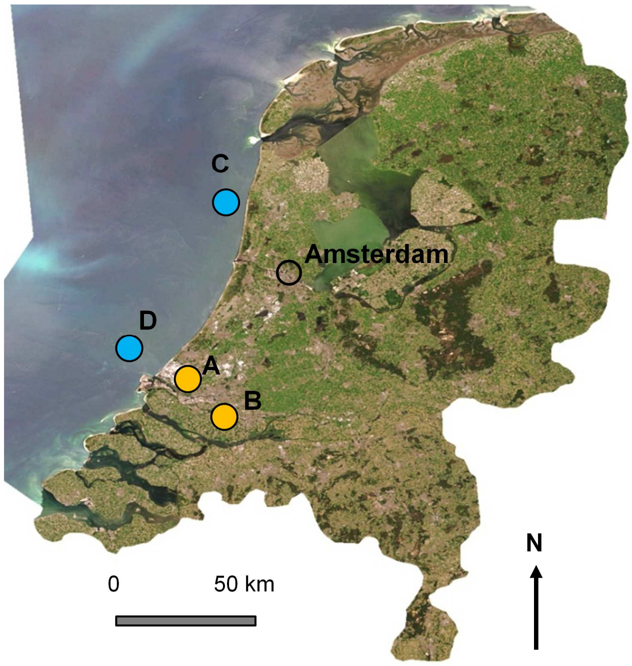

Fig. 1. Location of the potential CO_2 storage sites discussed in this paper. Legend: A - De Lier gas field; B – Barendrecht gas field; C – gas field in the Q8-A offshore block; D – gas field in the P-18 offshore block.

Table 1. Main characteristics of the sites.

Site	Reservoir depth [m]	Reservoir lithology	Cap rock lithology	Depletion [bar]
A	1350	Holland Greensand	Holland Marl	120
B	2630	Bunter Sandstone	Keuper Claystone	230
C	1700	Bunter Sandstone	Röt Claystone	140
D	3500	Bunter Sandstone	Röt Claystone, Evaporites	350

2. DEPLETION-INDUCED STRESS CHANGES AROUND DEPLETED RESERVOIRS

2.1. Method

The geomechanical effects of past hydrocarbon production and future CO_2 injection are frequently assessed by developing 2D, field scale, finite element (FE) models of the field under study. Typically, plain strain conditions are assumed, which restrict deformation to the 2D modeling plane. General drawback of a 2D modeling approach is that a strike-slip stress regime and strike-slip movement on faults can not be modeled. Also, in the case of small, compartmentalized reservoirs (a few kilometers to ten kilometers long and a few kilometers wide), the plane strain conditions may not, strictly speaking, apply. Nevertheless, a 2D modeling approach is often considered adequate for the phase of a feasibility study as the present day stress regime in the Netherlands is normal-faulting. An alternative and better approach of developing a 3D field-scale model of the storage site already in the feasibility phase of a CO_2 storage project is not common. Large part of additional cost related to 3D geomechanical modeling is the time-consuming construction of 3D meshes from structurally complex faulted framework models, for which no adequate industry standard software is readily available.

2D finite element models of the CO_2 storage sites presented in this paper are developed using a general-purpose FE program DIANA [11]. Each site-specific model is based on an interpreted seismic section converted from time to depth. The location and orientation of the cross-section is chosen in such a way as to enable evaluation of the maximum poro-mechanical effects on the caprock and faults. Favorable for a 2D approach is that the maximum horizontal stress direction is approximately aligned with the regional direction of the major axes of reservoir structures and faults. A representative 2D modeling section is then in a direction perpendicular to the maximum horizontal stress direction because:

- Both the maximum principal (vertical) stress and the minimum horizontal stress lie in the vertical modeling plane where the initial differential stresses are the largest and the effects of the induced stresses are also expected to be the largest.

- The largest true dip of faults is visible on the modeling plane. If reactivated in either normal- or reverse sense, the largest slip on a fault surface will occur in the direction of true dip.

The structural boundary conditions imposed on model boundaries constrain displacements perpendicular to the sides and base of the geomechanical model.

Differentiation of geomechanical units in the numerical models is based on a detailed lithological analysis of the reservoir, top seal and the overburden. Lithologies can often be resolved with a great degree of confidence using cut-offs on gamma-ray and sonic logs.

Experimental and field data on rock mechanics properties are often sparse, and other sources of information must be used to derive the values of material properties for all model units. Petrophysical well log interpretation is used to derive elastic rock properties; data from literature and other fields with similar lithology are also used.

Because we aim to assess the spatial extent of the net change in effective stresses at the end of depletion period, we re-run the selected site-specific models of CO_2 storage sites by applying the maximum pressure change to the reservoir based on the actual field data (Table 1). The effects of possible pressure drop in supporting aquifers is not taken into account because active aquifers are not present or very limited in areal extent due to faulting and compartmentalization.

We use linear elastic analysis and apply the pressure load only. This simple approach provides the first-order estimate of the extent of production-induced stress changes in and around a depleted reservoir, which is sufficient for our analysis. A more accurate and realistic prediction would require a non-linear analysis which takes into account additional effects due to non-linear reservoir compaction [e.g. 12, 13], stress relaxation in salt layers [e.g. 14, 15] and fault reactivation [e.g. 16]. These second-order non-linear models are more accurate in predicting the spatial pattern of local stress perturbations within the affected area, while the differences in the size of the affected area between the first-order and the second-order models are expected not to be significant. To delineate an area with stress changes from an area without (significant) stress change we use an arbitrary threshold of -0.1 MPa for compressive stresses and +0.1 MPa for tensile stresses.

2.2. Results and discussion

Field A

Field A is a simple anticlinal structure bounded by a reverse fault and a normal fault (Fig. 2). A 45m-thick gas reservoir is at a shallow depth of 1350 m. This case can be described as the case of a thin reservoir because the thickness-to-width ratio of the reservoir (i.e. the aspect ratio, *e*, is small, e= 0.016. The geomechanical model of Field A comprises 9 geomechanical units with different rock properties (Table 2).

Table 2. Mechano-stratigraphic units and their rock properties in the geomechanical model of Field A.

Geomechanical unit	Density [kg/m^3]	Elasticity modulus [GPa]	Poisson's coef. [-]
North Sea group	1960	0.25	0.38
Ommelanden chalk	2300	10	0.18
Upper Holland marl	2300	5.5	0.26
Middle Holland marl	2300	5.5	0.26
Greensand (gas res.)	2300	4.5	0.20
Lower Holland marl	2300	5.5	0.24
De Lier sand (oil res.)	2300	10.5	0.19
Vlieland claystone	2300	5.5	0.23
Rijswijk sandstone	2300	15	0.23

The largest induced stress changes at the end of depletion period occur in the caprock above the reservoir crest and at the abutments, around boundary faults (Fig. 3). The spatial pattern of stress changes is, however, asymmetric: in the west (left) abutment it is shifted above the reservoir due to the steeper inclination of the west reservoir flank and the presence of boundary fault. The extent of vertical and shear stress change is up to 1 km away from the reservoir (Fig. 3a,c). The area effected by induced horizontal stress change has the largest extent in the overburden - about 2.7 km, which is approximately equal to the reservoir width (Fig. 3b). This is likely due to the stiffness contrast between the soft uppermost North Sea sediments and the stiffer overburden layers beneath it, which take over most of the induced stresses from the uppermost soft layer.

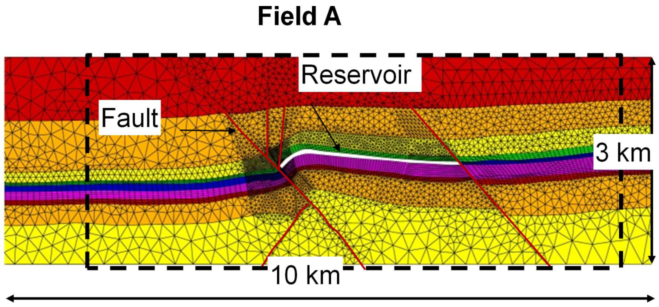

Fig. 2. Mesh for a 2D plane strain finite element model of Field A.

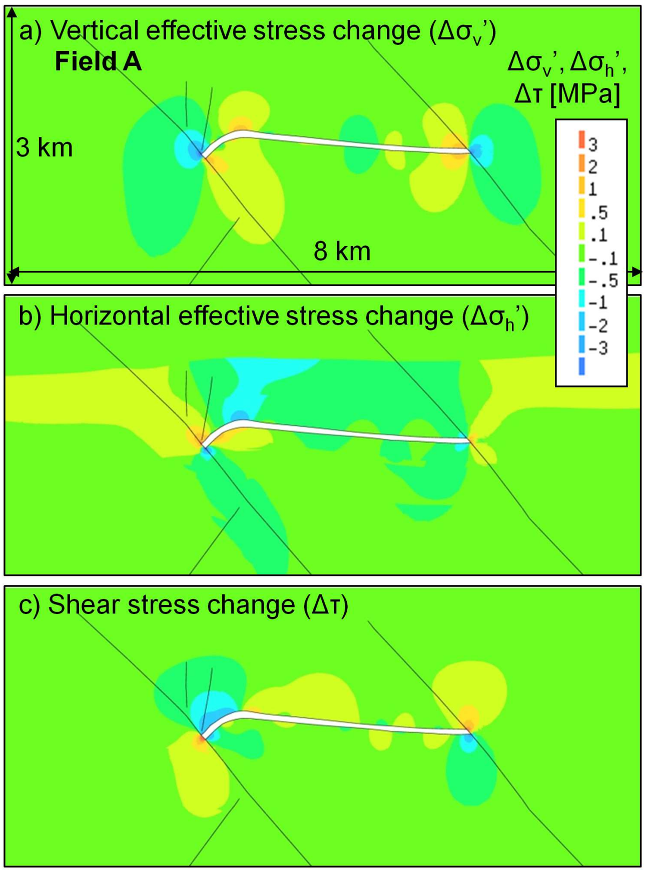

Fig. 3. Depletion-induced stress change in Field A. a) Vertical effective stress change; b) horizontal effective stress change, and c) shear stress change. Negative values indicate loading (i.e. compression).

Field B

Field B is a faulted block structure with over 200m-thick Bunter reservoir at a depth of 2630 m (Fig. 4). The structural blocks are bounded by faults which partly extend into the top seal. The reservoir aspect ratio is e=0.12, which is one order of magnitude larger than in the case of Field A. The geomechanical model of Field B comprises 12 geomechanical units with different rock properties (Table 3).

Table 3. Mechano-stratigraphic units and their rock properties in the geomechanical model of Field B.

Geomechanical unit	Density [kg/m^3]	Elasticity modulus [GPa]	Poisson's coef. [-]
North Sea group	1960	0.5	0.30
Chalk	2300	20	0.17
Rijnland	2650	15	0.25
Werkendam	2650	15	0.25
Posidonia shale	2650	15	0.25
Aalburg	2650	15	0.25
Up. Keuper claystone	2600	26	0.25
Up. Bunter (gas res.)	2600	20	0.35
Mid. Bunter (gas res.)	2600	12	0.35
Lower Bunter	2650	26	0.25
Upper Rotliegend	2600	20	0.35
Carboniferous	2650	30	0.25

The contour plots of different stress components reveal a pattern of stress transfer, i.e. stress arching (Fig. 5). Arching causes unloading (and decompaction) of the overburden above the reservoir and loading (i.e. an increase in the compressive stress) of the side-seal near the reservoir edges (Fig. 5a). The loaded part of the side-seal takes over part of the overburden load previously borne by the undepleted reservoir.

The extent of induced stress changes around the compacting reservoir is here larger than in the case of Field A. Vertical and shear stresses are perturbed within a distance equal to the width of the reservoir (Fig. 5a,c).

Induced shear stresses tend to concentrate at the edges of reservoir compartments, which represent weak spots susceptible to production-induced mechanical damage and possibly fault re-activation (Fig. 5c).

Horizontal stress changes affect larger areas than the vertical and shear stresses (Fig. 5b). Horizontal stresses tend to concentrate not only around the reservoir but also in the shallow overburden above the reservoir. The extent and magnitude of stress changes are larger than in the case of Field A because the stiffness of the overburden below the uppermost soft North Sea sediments in Field B is higher (E=15 to 26 GPa) than in the case of Feld A (E=4.5 to 10 GPa). The stiffer the overburden layer, the most likely it is to attract larger stress concentrations.

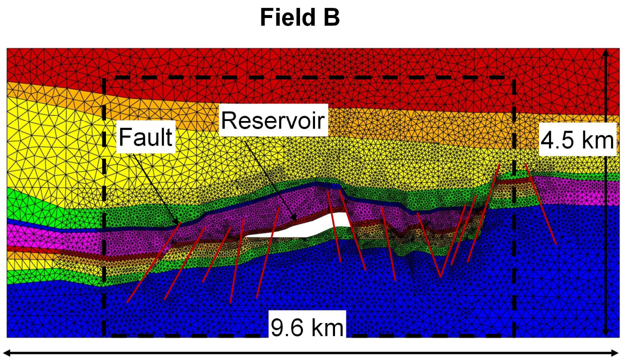

Fig. 4. Mesh for a 2D plane strain finite element model of Field B

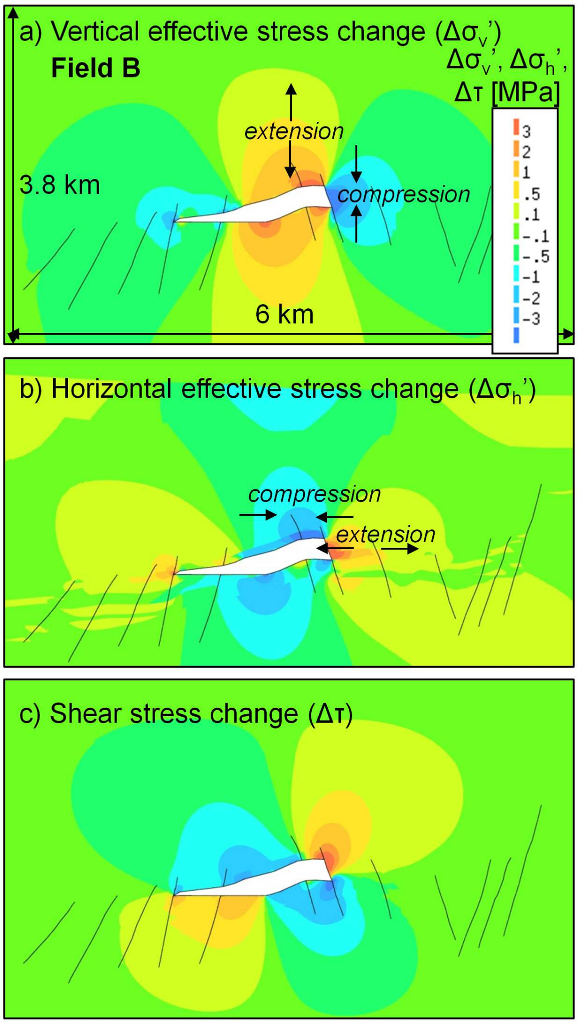

.

Fig. 5. Depletion-induced stress change in Field B. a) Vertical effective stress change; b) horizontal effective stress change, and c) shear stress change.

Field C

Field C represents a three way deep closure bounded by a fault structure to the southwest (left in Fig. 6). The field comprises two stacked sandstone reservoirs separated by a clay-siltstone layer. The total thickness of the Volpriehausen sandstone reservoir is about 60 m. The reservoir aspect ratio is e=0.07, which is in-between the values for Field A and B. The geomechanical model of Field C comprises 12 geomechanical units with different rock properties (Table 4).

Table 4. Mechano-stratigraphic units and their rock properties in the geomechanical model of field C.

Geomechanical unit	Density [kg/m^3]	Elasticity modulus [GPa]	Poisson's coef. [-]
North Sea group	1960	0.5	0.30
Aalburg	2650	15	0.25
Keuper, Muschelkalk	2650	22	0.25
Röt claystone	2650	18	0.25
Röt evaporite	2100	20	0.35
Low Röt claystone	2650	18	0.25
Solling sand (gas res)	2600	18	0.20
Volpriehausen clay	2650	19	0.25
Volpr. sand (gas res)	2600	14	0.20
Low. Buntsand. clay	2650	21	0.25
Zechstein	2100	20	0.35
Carboniferous	2650	30	0.25

The spatial pattern of stress perturbations at the end of reservoir depletion clearly shows the effects of stress transfer discussed previously (Fig. 7). Extent of the area affected by induced stress changes in the abutments is here limited to a distance less than the reservoir width (Fig. 7a,b). The areas affected by stress changes in the abutments are largely symmetric (with respect to the vertical axis through the reservoir crest) because the depleting reservoir has a shape of a simple anticlinal structure (Fig. 7a,b).

Extent of the area of horizontal stress changes affecting the caprock (above the reservoir) and the underburden (below the reservoir), is limited to a distance not exceeding the reservoir width. The pattern above the reservoir is, however, dissimilar to the pattern below the reservoir, which is due to different structural settings and mechanical rock properties of the overburden and the underburden (Fig. 7b). The uppermost soft North Sea sediments barely attract any depletion-induced stresses due to their low stiffness compared to the stiffness of the underlying overburden sediments.

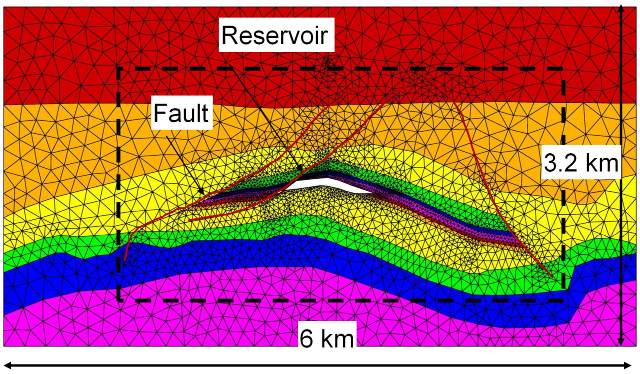

Fig. 6. Mesh for a 2D plane strain finite element model of Field C.

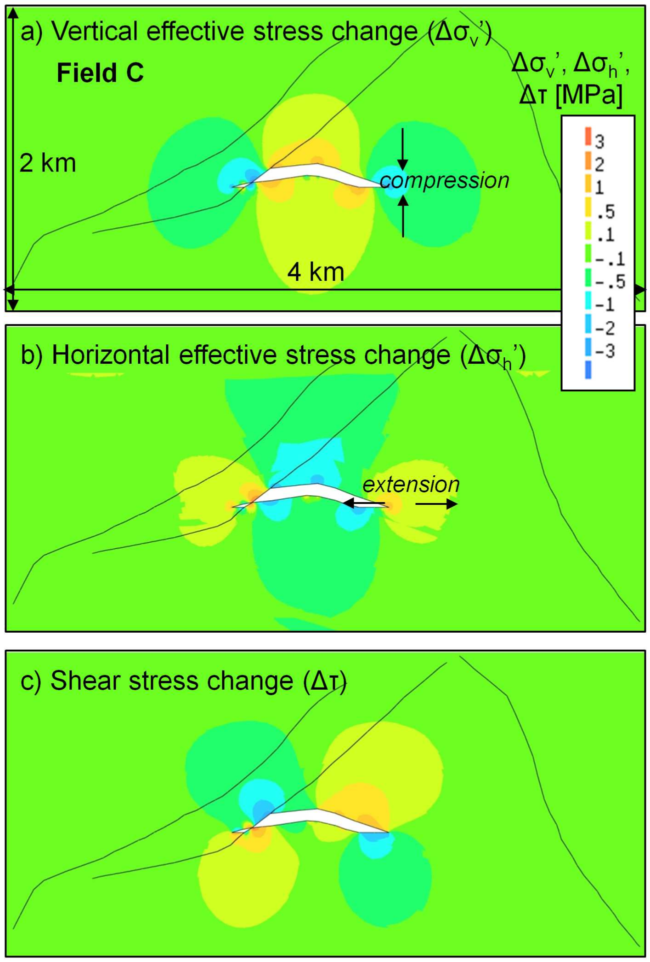

Fig. 7. Depletion-induced stress change in Field C. a) Vertical effective stress change; b) horizontal effective stress change, and c) shear stress change.

Field D

Field D consists of several fault bounded compartments (Fig. 8). It is the deepest reservoir considered in this study (3500 m) with reservoir thickness exceeding 200 m. The upper part of the Bunter reservoir (Hardegsen, Upper and Lower Detfurth) is the best part of the reservoir. The aspect ratio of this reservoir is e=0.12 (as in the case of Field B), assuming depletion in all three neighboring compartments. The geomechanical model of Field D comprises 12 geomechanical units with different rock properties (Table 4).

Table 5. Mechano-stratigraphic units and their rock properties in the geomechanical model of field D.

Geomechanical unit	Density [kg/m^3]	Elasticity modulus [GPa]	Poisson's coef. [-]
Up. North Sea group	1960	0.5	0.30
Low North Sea group	2600	5	0.30
Chalk	2300	20	0.17
Rijnland	2650	17	0.30
Schieland	2100	13	0.30
Altena	2600	15	0.30
Up. Germanic Trias.	2600	26	0.30
Detfurth (gas res)	2600	20	0.20
Volpriehaus. (gas res)	2600	25	0.20
Low. Germanic Trias.	2600	29	0.30
Zechstein	2100	20	0.35
Carboniferous	2650	30	0.25

The previously described general pattern of stress redistribution around the compacting reservoir can be observed (Fig. 9). In faulted reservoirs fault throw determines the degree of overlap between the faulted reservoir blocks and, accordingly, the degree of interference between the zones of induced stress changes caused by depletion of separate reservoir compartments. The superposition of stress changes induced by compaction of individual blocks can amplify the geomechanical effects on the caprock and faults.

The extent of induced stress changes around the compacting reservoir is here somewhat larger than in the previous cases. Vertical and shear stresses are perturbed within a distance 1.5 times the width of the reservoir (Fig. 9a,c).

Horizontal stress changes are clearly affected by the mechanical stratigraphy (i.e. differences in the elastic properties between the differentiated geomechanical units, Fig. 9b). Horizontal stress changes close to model boundaries are slightly influenced by the boundary conditions (i.e. horizontal displacements are constrained along the model sides). Hence, the predicted pattern of induced stress changes close to model boundaries may not be accurate. This can be corrected by placing the model boundaries further away from the compacting reservoir.

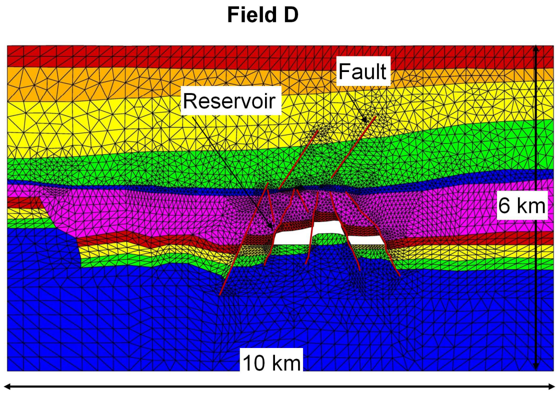

Fig. 8. Mesh for a 2D plane strain finite element model of Field D.

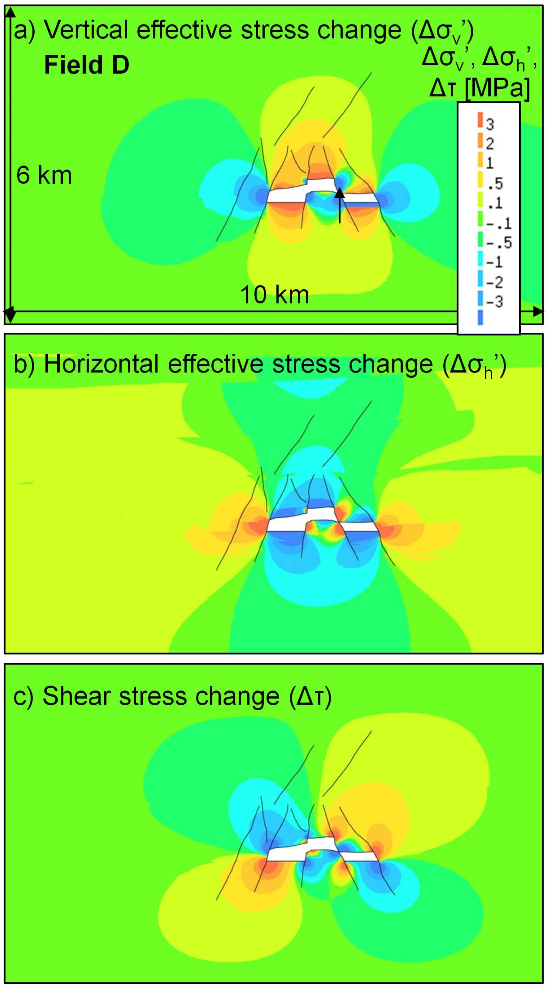

Fig. 9. Depletion-induced stress change in Field D. a) Vertical effective stress change; b) horizontal effective stress change, and c) shear stress change.

3. CONCLUSIONS

Geomechanical simulations were conducted on a number of site-specific numerical models of depleted gas fields considered for CO_2 storage in the Netherlands. Simulations were aimed at assessing the maximum areal extent of stress perturbation around depleted reservoirs without aquifer support at the end of depletion period. The simulations yielded the following conclusions:

- **(i)** The maximum extent of stress changes around depleting gas reservoirs is commonly one order of magnitude smaller than in the case of CO_2 storage in saline aquifers; typically, in the order of a few kilometers for gas reservoirs versus a few tens to hundreds kilometers for saline aquifers.
- **(ii)** The magnitude and pattern of induced stress changes depend on many factors, including the structural setting, reservoir shape, geomechanical properties and the stiffness contrast between the lithostratigraphic units.
- **(iii)** Typical spatial pattern of stress redistribution around a compacting reservoir comprises unloading of the overburden above the reservoir and loading of the side-seal near the reservoir edges.
- **(iv)** Depletion of structurally simple reservoirs, such as single compartment or anticlinal reservoirs, induces stress changes similar to the typical pattern. The areas affected by stress changes are largely symmetric with respect to the vertical axis through the crest of a reservoir.
- **(v)** In faulted, multi-compartment reservoirs, fault throw between the neighboring depleting blocks determines the degree of interference between the zones of induced stress changes caused by depletion of individual compartments.
- **(vi)** The superposition of stress changes can amplify the geomechanical effects. The top seal and boundary faults at the edges of reservoir compartments represent weak spots susceptible to production-induced mechanical damage and possibly fault re-activation.
- **(vii)** The extent of induced stress changes around the compacting reservoir depends on the aspect ratio, i.e. the thickness-to-width ratio of the reservoir (e).
- **(viii)** In the case of a small aspect ratio of the order of magnitude of $e \approx 0.01$, the extent of stress perturbations away from the reservoir edges is generally less than the reservoir width.
- **(ix)** In the case of a high aspect ratio of the order of $e \approx 0.1$, the extent of stress perturbations away from the reservoir edges is generally 1 to 1.5 times the reservoir width.

ACKNOWLEDGEMENTS

This research was conducted as part of the Dutch national project on CCS (CATO-2), which is supported by the Dutch government, and involves universities, private companies, and research institutes.

REFERENCES

1. The CATO-2 project website. 2013. http://www.co2-cato.org/cato-2/locations.

2. Hawkes, C., P.J. McLellan, U. Zimmer, and S. Bachu. 2004. Geomechanical factors affecting geological storage of CO_2 in depleted oil and gas reservoirs: risks and mechanisms. *Gulf Rocks 2004, 6th North American Rock Mechanics Symposium*, Houston, Texas, June 5-9, 2004, paper no 04-579.
3. Rutqvist, J., 2012. The geomechanics of CO_2 storage in deep sedimentary formations. *Geotechnical and Geological Engineering*. 30:3, 525-551.
4. Birkholzer, J.T., Q. Zhou, and C.-F. Tsang. 2009. Large-scale impact of CO_2 storage in deep saline aquifers: A sensitivity study on pressure response in stratified systems. *International Journal of Greenhouse Gas Control*. 3: 181-194.
5. Person, M., A. Banerjee, J. Rupp, C. Medina, P. Lichtner, C. Gable, R. Pawar, M. Celia, J. McIntosh, and V. Bense. 2010. Assessment of basin-scale hydrologic impacts of CO_2 sequestration, Illinois basin. *International Journal of Greenhouse Gas Control*. 4: 840-854
6. Orlic, B., J. ter Heege, and B.B.T. Wassing. 2010. Assessing the integrity of fault- and top seals at CO_2 storage sites. *Proceedings of the 10th International Conference on Greenhouse Gas Control Technologies* (GHGT-10). Amsterdam. Energy Procedia.
7. Hofstee, C., F. Seeberger, B. Orlic, F. Mulders, F. van Bergen, and R. Bisschop. 2008. The feasibility of effective and safe carbon dioxide storage in the De Lier gas field. *First Break*. 26, 53-57.
8. Orlic, B. 2009. Some geomechanical aspects of geological CO_2 sequestration. *KSCE Journal of Civil Engineering*. Korean Society of Civil Engineers (KSCE). 13: 225-232.
9. Shell CO_2 Storage Company B.V. 2008. *EIA Underground* storage *of CO_2 in Barendrecht* (in Dutch). Report no EP200809225671.
10. Arts, R., V.P. Vandeweijer, and C. Hofstee, M.P.D. Pluymaekers, D. Loeve, A. Kopp, W.J. Plug. 2012. The feasibility of CO_2 storage in the depleted P18-4 gas field offshore the Netherlands (the ROAD project). *International Journal of Greenhouse Gas Control*. 11: S10-S20.
11. TNO Diana. 2012. DIANA: *Finite element program and User Documentation*, version 9.4.3.
12. Dudley, J.W., A.J. van der Linden, and K.G. Mah. 2009. Predicting accelerating subsidence above the highly compacting Luconia carbonate reservoirs, offshore Sarawak Malaysia. *SPE Reservoir Evaluation & Engineering.* 12:104-115.
13. De Gennaro, S., P. Schutjens, P. Frumau, M. Fuery, J. Ita, and P. Fokker. 2010. The role of geomechanics in the development of an HPHT field. In *Proceedings of the 44th US Rock Mechanics Symposium, Salt Lake City, 27-30 June 2010*, paper no ARMA 10-450.
14. Schutjens P.M., J.R. Snippe, H. Mahani, J. Turner, J. Ita and A.P. Mossop. 2010. Production-induced stress change in and above a reservoir pierced by two salt domes: a geomechanical model and its applications. In *Proc. SPE EUROPEC/EAGE Annual Conference and Exhibition*, Barcelona, Spain, 14-17 June 2010, SPE paper 131590.
15. Orlic, B. and B.B.T. Wassing. 2013. A study of stress change and fault slip in producing gas reservoirs overlain by elastic and viscoelastic caprocks. *Rock Mechanics and Rock Engineering*. 46:421-435.
16. Alassi, H., R. Holt, and M. Landrø. 2010. Relating 4D seismics to reservoir geomechanical changes using a discrete element approach. *Geophysical Prospecting*. 58:657-668.